

of biotin to bicarbonate is related to a cyclization reaction reported by Blagoeva and co-workers.¹⁴ Our work establishes that the tetrahedral adduct of bicarbonate and biotin should react readily with an adjacent phosphate. Such a process, when considered in both forward and reverse directions, is reasonable in comparison with other mechanisms. The reverse reaction involves the attack of phosphate on carboxybiotin, which is analogous to the transfer of the carboxyl group to acceptors in the normal carboxylation process. In the forward direction, the phosphate ester thus generated will decompose by expulsion of the phosphate from the carbonyl hydrate to generate the carbonyl. The parallel reactions are shown in Scheme V.

How Is Biotin Really Carboxylated? The mechanism of carboxylation of biotin remains to be discovered, and experiments to rule out or confirm any mechanism need to be developed. Jencks has proposed that organic reactions "choose" their mechanism simply by finding the lowest energy stepwise pathway involving stable intermediates.⁴³ On the other hand, the choice of mechanism of an enzyme-catalyzed reaction depends on the structure of the enzyme and the pathway through which the enzyme evolved.^{44,45} Evolutionary pressures can direct the development of a pathway without necessarily leading to the overall most rapid pathway if other considerations related to efficiency within the environment take precedence. Consistent with such expectations, biochemical studies are usually aimed at discovering a reaction rather than deducing how a reaction occurs. In this context, what advantages would cause this mechanism to be fa-

vored? First, the efficient utilization of ATP is normally an important evolutionary consideration. If ATP is cleaved, it should always lead to formation of the product; otherwise, metabolic processes that led to the generation of ATP will be wasted and the organism will be obliged to provide a new source of energy to permit recoupling of ADP and phosphate. In the present mechanism, as in others, the cleavage of ATP is in a step that produces another intermediate whose reaction is heavily favored toward formation of the product, carboxybiotin. By comparison, mechanisms in which ATP first reacts with bicarbonate to produce carboxyphosphate generate a species that will produce carbon dioxide rapidly.⁷ This must be trapped since the lifetime of carboxyphosphate is inherently short.⁷ Having the reaction with bicarbonate occur first requires no commitment of ATP until after reaction with bicarbonate has occurred. Thus, the system can be efficient in providing a direct route to utilize the most abundant species.

Conclusions. Our results show that the reaction patterns of dialkyl phosphate esters 1-3 are consistent with mechanisms that involve the reaction of the carbonyl hydrate and the internal phosphate ester. The resulting intermediate reacts at phosphorus and then decomposes via C-O cleavage to form the ketone and expel the dialkyl phosphate ester. The latter process serves as a model for proposed reaction of the adduct of biotin and bicarbonate, which is completed by reaction with ATP to form carboxybiotin. It remains to test the mechanism in an enzymic system where key transition states can serve as targets of probes that provide the necessary differentiation.

Acknowledgment. We thank the Natural Sciences and Engineering Research Council of Canada for support through an operating grant and for a postgraduate fellowship to S.D.T.

(43) Ta-Shama, R.; Jencks, W. P. *J. Am. Chem. Soc.* **1986**, *108*, 8040.

(44) Albery, W. J.; Knowles, J. R. *Acc. Chem. Res.* **1977**, *10*, 105.

(45) Benner, S. A.; Nambiar, K. P.; Chambers, G. K. *J. Am. Chem. Soc.* **1985**, *107*, 5513.

Tetraarylethanedioles: Surprisingly Low Energy Requirements for Electron Transfer in Solution and in the Gas Phase

John H. Penn,* Zhe Lin, and Dao-Li Deng

Contribution from the Department of Chemistry, West Virginia University, Morgantown, West Virginia 26506-6045. Received November 2, 1989

Abstract: A number of methyl-substituted tetraarylethanedioles **1** have been found to undergo facile electron transfer (et) to tris(1,10-phenanthroline)iron(III) complexes ($\text{Fe}^{\text{III}}\text{L}_3$). The products of this reaction are the corresponding benzophenones when an appropriate base is added to the reaction solution. The electron-transfer rate constants (k_{et}) for the reaction of **1** and $\text{Fe}^{\text{III}}\text{L}_3$ have been measured as a function of temperature and are higher than anticipated, based on the energetic predictions derived from model arenes. The oxidation potential, derived from the measured ΔG_{et}^* , is in good agreement with the solution-phase $\Delta G_{\text{et}}^\circ$, which can be calculated from the gas-phase ionization potential. Control experiments demonstrate that the reaction proceeds through a normal outer-sphere electron-transfer reaction. The surprisingly low oxidation potentials can only be explained by through-space phenyl-phenyl interactions.

Introduction

There has been much recent activity directed toward understanding the reactivity of radical cations. The utility of radical cations in organic chemistry has been demonstrated in their use in photochemically¹⁻⁴ and thermally⁵ induced electron-transfer

bond-cleavage reactions, thermally activated cycloaddition reactions,⁶ and a variety of other electrocyclic reactions.⁷⁻¹⁰ Our general interest in bond-cleavage reactions has stimulated our

(4) (a) Davis, H. F.; Das, P. K.; Griffin, G. W. *J. Am. Chem. Soc.* **1984**, *106*, 6968. (b) Reichel, L. W.; Griffin, G. W.; Muller, A. J.; Das, P. K.; Ege, S. N. *Can. J. Chem.* **1984**, *62*, 424.

(5) Camaioni, D. M.; Franz, J. A. *J. Org. Chem.* **1984**, *49*, 1607.

(6) (a) Chockalingam, K.; Pinto, M.; Bauld, N. L. *J. Am. Chem. Soc.* **1990**, *112*, 447. (b) Bauld, N. L. *Tetrahedron*, **1989**, *45*, 5307 and references therein.

(7) Roth, H. D. *Acc. Chem. Res.* **1987**, *20*, 343 and references therein.

(8) Gassman, P. G.; Bonser, S. M.; Mlinaric-Jajerski, K. *J. Am. Chem. Soc.* **1989**, *111*, 2652.

(9) (a) Williams, F.; Guo, Q. X.; Nelsen, S. F. *J. Am. Chem. Soc.* **1990**, *112*, 2028. (b) Nelsen, S. F.; Teasley, M. F. *J. Org. Chem.* **1989**, *54*, 2667.

(10) Arnold, D. R.; Mines, S. A. *Can. J. Chem.* **1987**, *65*, 2312.

(1) (a) Popielarz, R.; Arnold, D. R. *J. Am. Chem. Soc.* **1990**, *112*, 3068. (b) Arnold, D. R.; Lamont, L. J. *Can. J. Chem.* **1989**, *67*, 2119.

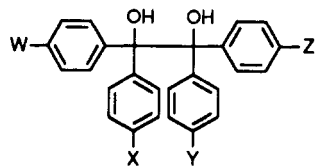
(2) (a) Bergmark, W. R.; Whitten, D. G. *J. Am. Chem. Soc.* **1990**, *112*, 4042. (b) Haugen, C. M.; Whitten, D. G. *J. Am. Chem. Soc.* **1989**, *111*, 7281.

(c) Kellett, M. A.; Whitten, D. G. *J. Am. Chem. Soc.* **1989**, *111*, 2314. (d) Ci, X.; Silveira da Silva, R.; Nicodem, D.; Whitten, D. G. *J. Am. Chem. Soc.* **1989**, *111*, 1337. (e) Ci, X.; Whitten, D. G. *J. Am. Chem. Soc.* **1987**, *109*, 7215.

(3) (a) Maslak, P.; Chapman, W. H., Jr. *J. Chem. Soc., Chem. Commun.* **1989**, 1809. (b) Maslak, P.; Asel, S. L. *J. Am. Chem. Soc.* **1988**, *110*, 8260.

interest in those compounds that undergo photochemically induced electron-transfer-initiated bond-cleavage reactions. For these compounds, extremely low radical-cation bond dissociation energies have been postulated to be the main reason that efficient bond cleavage occurs.^{2c} We hoped to exploit these low bond dissociation energies to learn more about endergonic electron-transfer (et) processes,¹¹⁻¹⁵ with the ultimate aim of better understanding oxidation processes and fossil fuel conversion reactions.

For radical cations having very low bond dissociation energies, the overall bond-cleavage rate in an et reaction will be controlled solely by the et rate (k_{et}), since the et process requires much more energy than dissociation. Although this general strategy has been previously used to determine k_{et} in isolated systems,^{11c,16} we hoped that the general application of this strategy would allow new insight into the molecular requirements controlling endergonic et processes. For our early research efforts directed toward evaluating the potential of this general methodology for determining endergonic et rates, arylpinacols were chosen to be the electron donors because their radical cations are known to cleave at a rapid rate^{4,17} and their oxidation potentials may be tuned through proper choice of substituents. Tris(1,10-phenanthroline)iron(III) complexes ($Fe^{III}L_3$) were chosen to be the electron acceptors because $Fe^{III}L_3$ complexes undergo electron transfer through an outer-sphere mechanism,¹⁸ have absorptions in the visible region allowing for facile concentration measurements, and have well-known reduction potentials, which may be varied systematically by proper choice of the phenanthroline substituents.¹⁹ During our et rate studies, we observed unusually rapid electron-transfer rates from 1,1,2,2-tetrahydroethane-1,2-diol (**1a**) to $Fe^{III}L_3$. We report here our studies designed to understand these rapid et rates. The methylated derivatives of **1** shown below were specifically chosen because their rates could be measured conveniently and the placement of the methyl groups in these compounds would allow an evaluation of various phenyl-phenyl interaction modes.



compd	W	X	Y	Z
1a	H	H	H	H
1b	CH ₃	H	H	H
1c	CH ₃	CH ₃	H	H
1d	CH ₃	H	CH ₃	H
1e	CH ₃	CH ₃	CH ₃	CH ₃

Results

Starting-Material Synthesis. Compounds **1a,c,e** were synthesized by standard photochemical methods. Compounds **1b,d** were synthesized by addition of the appropriate Grignard reagent(s) to benzil. Prior to kinetic analysis, all compounds used in this study were recrystallized three times from hexane/ethyl

(11) (a) Ebersson, L.; Ekstroem, M. *Acta Chem. Scand.* **1989**, *43*, 86. (b) Svensson, C.; Albertsson, J.; Ebersson, L. *Acta Chem. Scand., Ser. B* **1988**, *B42*, 596. (c) Ebersson, L.; Ekstroem, M. *Acta Chem. Scand., Ser. B* **1987**, *B41*, 41.

(12) (a) Kochi, J. K. *Angew. Chem.* **1988**, *27*, 1227. (b) Schlesener, C. J.; Amatore, C.; Kochi, J. K. *J. Phys. Chem.* **1986**, *90*, 3747.

(13) (a) Schlesener, C. J.; Amatore, C.; Kochi, J. K. *J. Am. Chem. Soc.* **1984**, *106*, 3567. (b) Schlesener, C. J.; Kochi, J. K. *J. Org. Chem.* **1984**, *49*, 3142.

(14) Baciocchi, E.; Del Giacco, T.; Murgia, S. M.; Sebastiani, G. V. *J. Chem. Soc., Chem. Commun.* **1987**, 1246.

(15) Reed, R. A.; Murray, R. W. *J. Phys. Chem.* **1986**, *90*, 3829.

(16) Fukuzumi, S.; Wong, C. L.; Kochi, J. K. *J. Am. Chem. Soc.* **1980**, *102*, 2928.

(17) Sankararaman, S.; Perrier, S.; Kochi, J. K. *J. Am. Chem. Soc.* **1989**, *111*, 6448.

(18) Wong, C. L.; Kochi, J. K. *J. Am. Chem. Soc.* **1979**, *101*, 5593.

(19) (a) Dulz, G.; Sutin, N. *Inorg. Chem.* **1963**, *2*, 917. (b) Diebler, H.; Sutin, N. *J. Phys. Chem.* **1964**, *68*, 174. (c) Wilkins, R. G.; Yelin, R. E. *Inorg. Chem.* **1968**, *7*, 2667.

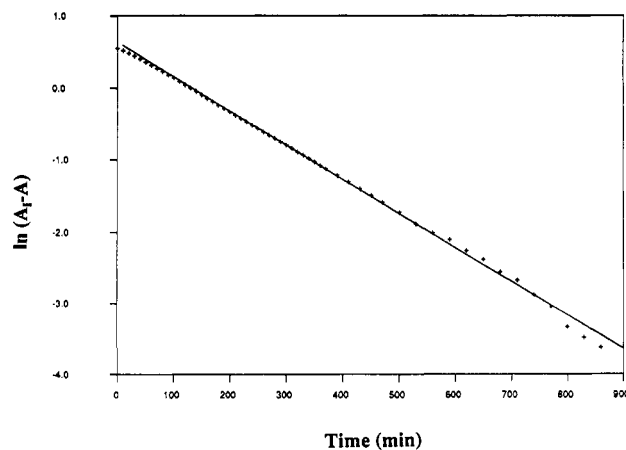


Figure 1. Typical kinetic experiment for the appearance of $Fe^{II}L_3$ with 0.01 M **1a** and 2.5×10^{-3} M DBP at 40 °C.

Table I. Product Analyses

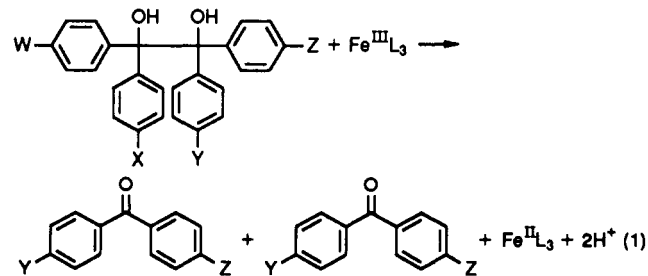
substr	substr concn (M)	base concn (mM)	ketone product yield (mole %)	reactn time (h)	reactn temp (°C)
1a ^a	0.01	DBP 5.0	190	2	50
1d	0.01	DBP 2.5	198	1	40
1e	0.01	DBP 2.5	197	1	50

^a Reference 20.

acetate. HPLC analysis showed these compounds to be uncontaminated by other isomers of **1**. For further details of the syntheses, see the Experimental Section.

Product Determinations. Product analyses for the oxidation reactions of pinacols and $Fe^{III}L_3$ in acetonitrile solution have been previously reported.²⁰ In the absence of an appropriate base, **1a** yields a mixture of benzophenone, tetraphenylloxirane, and triphenylacetophenone. In contrast, when either 2,6-di-*tert*-butylpyridine (DBP) or 4-cyanopyridine (4CP) is added to the reaction solution, the acid rearrangement products are eliminated, leaving only benzophenone as a product.²⁰

Although we believed that these oxidation reactions resulted only in the corresponding ketones on the basis of our previous work, we have made product determinations for two additional isomers of **1** to further substantiate our claim that the kinetics of the observed reaction correspond only to a simple outer-sphere et reaction. HPLC analyses of the reaction mixtures have been performed for **1d,e**, with the results of the quantitative analysis shown in Table I. Clearly, quantitative production of the corresponding ketones is observed for these symmetrical pinacols. Therefore, the reaction of **1** with $Fe^{III}L_3$ is described by eq 1.



Electron-Transfer Rate Measurements. Our strategy for determining k_{et} is based on a rate-determining et step^{11c,16} in which all reactions subsequent to the initial electron transfer are more rapid than the initial et event. The reaction rates were determined by monitoring the concentration of $Fe^{II}L_3$ at 506 nm. With a large **[1]** relative to **[Fe^{III}L₃]**, pseudo-first-order kinetic behavior was observed for the appearance of $Fe^{II}L_3$ over a period of 3–5

(20) Penn, J. H.; Deng, D.-L.; Chai, K.-J. *Tetrahedron Lett.* **1988**, *29*, 3635.

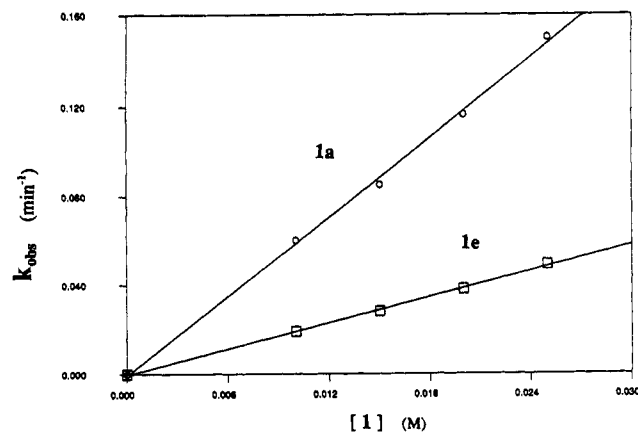


Figure 2. Observed reaction rate as a function of the concentration of **1** (**1a** measured at 70 °C; **1e** measured at 30 °C).

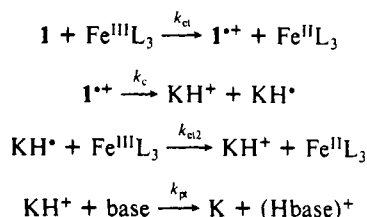
half-lives. Note Figure 1 for typical data.

The product determination studies suggested that base in the solution may influence the observed reaction rate. In accord with this expectation, the observed rate of reaction of **1a** diminished from $3.97 \times 10^{-5} \text{ s}^{-1}$ to $3.42 \times 10^{-5} \text{ s}^{-1}$ upon the addition of 2.5 mM DBP to the solution. However, the addition of further DBP (0.01 M) resulted in no further decrease in the observed rate. In addition, the observed rates were independent of the base used, since both DBP and 4CP gave identical rates. Therefore, all rate determinations were made with 2.5–10 mM base added to the solution.²¹

Several control experiments allow us to evaluate the kinetic order of each reagent. Separate experiments used to monitor the rate of disappearance of $\text{Fe}^{\text{III}}\text{L}_3$ produced data within experimental error of the rates of appearance of $\text{Fe}^{\text{II}}\text{L}_3$. No reduction of $\text{Fe}^{\text{III}}\text{L}_3$ occurred unless **1** was added to the solution. The observed rate was identical for two different initial concentrations of $\text{Fe}^{\text{III}}\text{L}_3$, eliminating the possibility that the observed kinetics are influenced by long-lived radical cations that may undergo reverse et with the $\text{Fe}^{\text{II}}\text{L}_3$ being produced in the reaction. We conclude that the reaction rate is kinetic first-order in $\text{Fe}^{\text{III}}\text{L}_3$. The reaction rate was confirmed to be kinetic first-order in **1** by plotting k_{obs} as a function of concentration for **1a,e** as shown in Figure 2. Although these rate studies were conducted at two different temperatures, the data are clearly in accord with the reaction being kinetic first-order in **1**.

The et rate constants were derived with eq 2, based on the kinetic analysis shown in Scheme I. Initial et from **1** to $\text{Fe}^{\text{III}}\text{L}_3$ yields $\text{I}^{*\cdot}$ with rate constant k_{et} . Cleavage of $\text{I}^{*\cdot}$ (rate constant

Scheme I. Kinetic Analysis Used for Electron-Transfer Rate Determinations



k_{c}) yields a ketyl radical (KH^{\cdot}) and a protonated ketone (KH^+). KH^{\cdot} is oxidized by another $\text{Fe}^{\text{III}}\text{L}_3$ to yield a second KH^+ with rate constant $k_{\text{et}2}$. Since the oxidation of benzylic radicals by $\text{Fe}^{\text{III}}\text{L}_3$ has previously been shown to be a kinetically fast process relative to the initial et process from aromatics,¹³ we assume that the more electron-rich KH^{\cdot} will be oxidized in a kinetically fast step. The protonated ketones react with the added base to yield

(21) The observed reaction rate was very dependent on residual water in the solution with $10^{-3} \text{ M H}_2\text{O}$ causing a ca. 50× acceleration in the observed reaction rate. This prevented our determination of salt effects or maintaining a constant ionic strength of the solution.

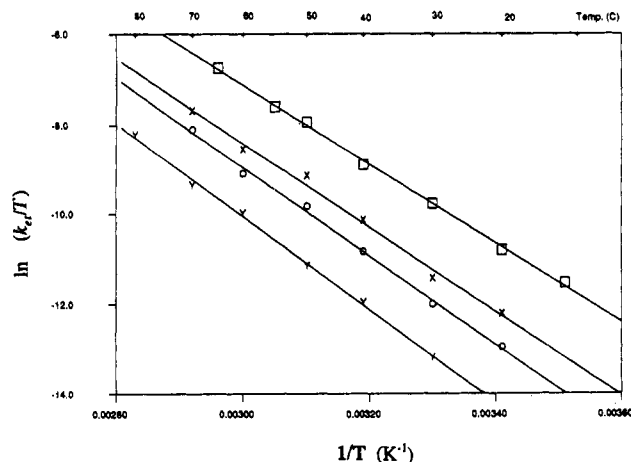


Figure 3. Temperature dependence of the electron-transfer rates (Y, **1a**; O, **1b**; X, **1c,d**; □, **1e**).

Table II. Activation Parameters for the Electron Transfer to $\text{Fe}^{\text{III}}\text{L}_3$

parameter	1a	1b	1c	1d	1e
ΔH^\ddagger (± 0.5 kcal/mol)	20.6	19.6	18.7	18.7	17.6
ΔS^\ddagger (± 1.5 cal/mol °K)	-5.3	-6.2	-7.8	-7.8	-9.0
ΔG_{30}^\ddagger (± 0.1 kcal/mol)	22.1	21.5	21.1	21.1	20.2
k_{et}^{30} ($\times 10^{-3} \text{ M}^{-1} \text{ s}^{-1}$)	1.1	3.1	6.0	6.0	26.8
temp range (°C)	30–80	20–70	20–70	20–70	15–65

Table III. Thermodynamic Data

parameter	1a	1e	3
IP (eV)	8.42 ± 0.02	8.35 ± 0.05	9.01 ± 0.02
E_{ox}° (V vs SCE) ^a	1.88	1.83	2.30
$E_{\text{ox}(p)}^\circ$ (V vs Fe(II) complex)	1.08		1.14
ΔG_{30}° (kcal/mol) ^b	18.2	17.0	27.8

^a Calculated with eq 3. ^b Calculated with eq 4.

another ketone in another kinetically fast step. If $k_{\text{et}}[\text{Fe(III)}] \ll k_{\text{c}}$, then the rate-determining step of the reaction will be $k_{\text{et}}[\text{Fe(III)}]$, i.e., the initial et step.

$$k_{\text{obs}} = 2k_{\text{et}}[\mathbf{1}] \quad (2)$$

Measurement of k_{et} over a 50 °C temperature range for each isomer of **1** has allowed the determination of activation parameters for et from **1** to $\text{Fe}^{\text{III}}\text{L}_3$. These data are shown in Figure 3 and gathered in Table II. Of particular note is that the rates of **1c,d** were found to be identical within experimental error for all temperatures.

Calculation of ΔG° for the Electron-Transfer Reaction. Ultimately, the ideal correlation of reactivity would involve a direct comparison of the kinetic data (evaluation of the energetics of the transition state) and thermodynamic data (evaluation of the energetics of the isolated species). The kinetic data have been described above. The corresponding thermodynamic data could, in principle, be obtained from the measurement of reversible electrode potentials. However, our reaction scheme's requirement for the radical cations to have kinetically fast reactions makes the measurement of reversible electrode potentials nearly impossible. Therefore, we have relied on a secondary technique to provide an estimate of the solution-phase oxidation potential.

In an elegant study, Kochi and Wightman²² have reported a correlation of the reversible solution-phase oxidation potentials (E_{ox}°) for a large number of polynuclear aromatic compounds and their methylated derivatives with the gas-phase ionization potential (IP) (as determined by ultraviolet photoelectron spectroscopy (UPS)). For acetonitrile, this correlation is given by eq 3, where E_{ox}° is the oxidation potential in acetonitrile solution (V) relative to SCE and IP is the UPS ionization potential (eV).

(22) Howell, J. O.; Goncalves, J. M.; Amatore, C.; Klasing, L.; Wightman, R. M.; Kochi, J. K. *J. Am. Chem. Soc.* **1984**, *106*, 3968.

$$E_{\text{ox}}^{\circ} = 0.71\text{IP} - 4.10 \quad (3)$$

In order to estimate E_{ox}° , the gas-phase IPs of **1a,e** were determined by UPS. Surprisingly, as can be seen in Table III, **1a,e** are much easier to oxidize than toluene (8.65 eV) and have IPs similar to that of the trialkyl 1,3,5-trimethylbenzene (8.42 eV).²² To verify that the surprisingly low IP was not due to an electron-donating effect of the hydroxy groups of **1**, the IP of *d,l*-2,3-diphenyl-2,3-butanediol (**3**) was also measured (Table III). The ΔIP between **1a** and **3** of 0.59 V (13.6 kcal/mol) clearly indicates that **1a** is much easier to oxidize than anticipated.

Further support for the facile oxidation of **1** is shown by the irreversible $E_{\text{ox(p)}}$ for **1a** and **3** (Table III). Although the uncertainties of the irreversible electrode potentials minimize the $\Delta E_{\text{ox}}^{\circ}$ between **1a** and **3**, **1a** is still easier to oxidize than **3**, in agreement with the IP measurements described above.

An estimate of ΔG° for the et reaction from **1** to $\text{Fe}^{\text{III}}\text{L}_3$ may be calculated with eq 4, where E° is the reversible solution-phase redox potential for the appropriate half-reaction and F is the Faraday constant. ΔG_{30}° is then calculated with use of $E_{\text{red}}^{\circ}(\text{Fe}^{\text{III}}\text{L}_3) = 1.09$ V vs SCE^{13a} and the $E_{\text{ox}}^{\circ}(\mathbf{1})$ data in Table III. These data are also gathered in Table III.

$$\Delta G_{30}^{\circ} = F(E_{\text{ox}}^{\circ}(\mathbf{1}) - E_{\text{red}}^{\circ}(\text{Fe}^{\text{III}}\text{L}_3)) \quad (4)$$

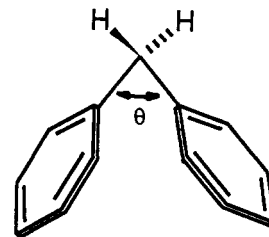
Calculated Ionization Potentials. The unexpectedly low IP and E_{ox}° for **1**, relative to those of monoalkyl-substituted arenes (vide infra), caused us to attempt to understand the origin of these effects from a molecular standpoint. Since phenyl-phenyl interactions (Ph-Ph interactions) appeared to be important, we have calculated the changes in IP with changes in molecular structure through the use of semiempirical calculations of the IP for various kinds of Ph-Ph interactions. For these calculations, the AM-1 method²³ was chosen because of its ability to reproduce experimental IP data. We emphasize that our calculated IPs are not intended to reproduce experimental IPs exactly but are intended to provide theoretical support to the idea that possible interaction modes can lead to IP lowering.

Our approach to understanding the nature of various Ph-Ph interactions and their effect on the electronic structure of **1** was to calculate the IP for specific bibenzyl and diphenylmethane geometries. These molecules are small enough to permit reasonable computation times, while geometrical changes can be enforced on these molecules through appropriate selection of bond angles and lengths. In this way, the calculated IPs can be compared to the calculated ΔH_f° for certain interactions.

To facilitate our discussion of possible Ph-Ph interactions, we will use the symmetry designations of the benzene π orbitals. In benzene, the HOMO orbitals are doubly degenerate e_{1g} orbitals. When a substituent is added to benzene (e.g., toluene), the degeneracy is removed, giving rise in C_{2v} symmetry to an a_2 orbital, which has a node at the position of the substituent, and a b_1 orbital, which interacts strongly with the substituent through the large magnitude of the wave function at the point of substitution.

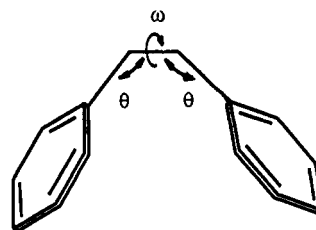


We anticipated that enforced interaction of the phenyl groups would lead to through-space interactions, leading to changes in the MO energies, which in turn would affect the IP of the molecule. For the proper geometry, the a_2 orbitals of one phenyl group may interact with the a_2 orbitals of the second phenyl group, removing the degeneracy of the two a_2 orbitals that would be obtained at infinite separation. Similar arguments hold for the



θ	IP (eV)	ΔH_f° (kcal/mole)
115.0	9.31	42.23
112.8	9.31	42.19
110.0	9.26	42.51
105.0	9.20	44.01
100.0	9.12	47.11
95.0	9.01	51.79

Figure 4. Effect of 1,1-phenyl-phenyl interactions on the IP.



θ	Eclipsed Conformation ($\omega=0^{\circ}$)		Gauche Conformation ($\omega=60^{\circ}$)	
	IP (eV)	ΔH_f° (kcal/mole)	IP (eV)	ΔH_f° (kcal/mole)
120	9.26	40.82	9.23	38.40
115	9.26	40.40	9.25	36.94
110	9.10	43.24	9.27	38.21
107.5	8.97	46.71	9.26	40.16
105	8.82	52.17	9.16	43.31
100	8.52	69.78	8.86	56.25

Figure 5. Effect of 1,2-phenyl-phenyl interactions on the IP.

b_1 orbitals. The magnitude of the splitting of these orbital energy levels from the symmetric and antisymmetric combinations of these orbitals would be a function of the through-space interactions of the phenyl groups, with greater interactions resulting in a greater splitting of the orbital energies. If the HOMO of the molecule originated from the antisymmetric combination of the a_2 - a_2 orbitals or the b_1 - b_1 orbitals, then a greater through-space interaction would result in a higher HOMO energy with a resultant decrease in the IP. These expectations have been realized in the calculations described below.

Our modeling of 1,1-Ph-Ph interactions is shown in Figure 4. The calculated minimum-energy geometry of diphenylmethane has a bond angle (θ) between the phenyl rings of 112.8° . The effect of steric compressions forcing the phenyl rings together was modeled by decreasing θ while allowing all other bond lengths and angles except θ to be optimized during the course of the calculation. As expected, the IP does indeed decrease as the phenyl rings are pushed more closely together. Surprisingly, the overall change in energy in the molecule due to steric interactions increases only modestly relative to the changes in the IP. An IP decrease of 0.30 eV (6.9 kcal/mol) is observed with only a 9.6 kcal/mol increase in ΔH_f° ($\theta = 95^{\circ}$).

Our modeling of 1,2-Ph-Ph interactions is shown in Figure 5. Here the situation is more complex, since the dihedral angle of the phenyl groups (ω) must be considered in addition to the torsional angle (θ) changes. In these calculations, the angle of the phenyl groups relative to the benzylic C-C σ bond must also be fixed in order to avoid twisting of the phenyl groups due to the steric interactions of the two phenyl groups during energy minimization. Our calculations include the eclipsed conformation ($\omega = 0^{\circ}$) and the gauche conformation ($\omega = 60^{\circ}$) since different

(23) Dewar, M. J. S.; Zoebisch, E. G.; Healy, E. F.; Steward, J. J. P. *J. Am. Chem. Soc.* **1985**, *107*, 3902.

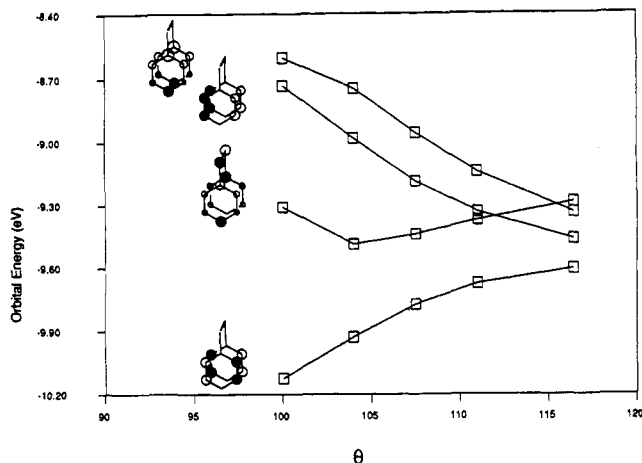


Figure 6. Orbital energies as a function of θ for the eclipsed conformation of bibenzyl.

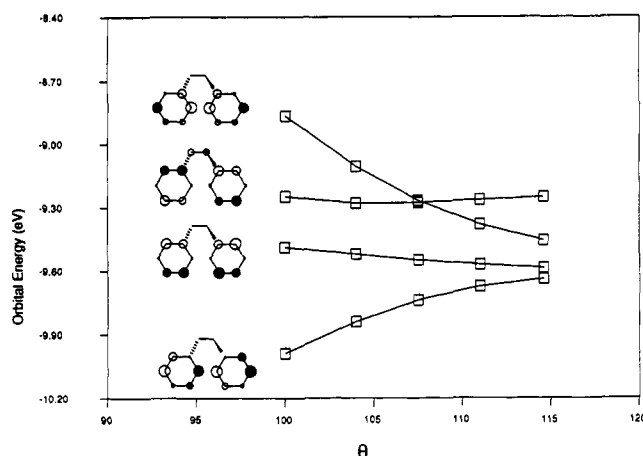


Figure 7. Orbital energies as a function of θ for the gauche conformation of bibenzyl.

through-space interactions would be anticipated for these two conformations. The results of these calculations reveal that significant IP decreases can be obtained with only modest increases in steric energy.

Following the molecular orbital energy levels of the highest occupied molecular orbitals is particularly instructive for these calculations on 1,2-Ph-Ph interactions. The four highest energy occupied orbital energies (and their corresponding wave functions) as a function of θ are shown in Figure 6 for the eclipsed conformation. At the optimized geometry ($\theta \approx 115^\circ$), the HOMO is an orbital containing a large amount of hyperconjugation through the benzylic C-C σ bond. As θ is varied, the energy of this orbital does not change dramatically. The second and third highest MOs are the antisymmetric combination orbitals of the b_1 and the a_2 orbitals, respectively. As anticipated, the energies of these orbitals are particularly sensitive to θ , with decreasing θ leading to higher orbital energies and lowered IPs. As seen in Figure 5, a Δ IP of 0.29 eV (6.7 kcal/mol) can be effected with an overall molecular energy change ($\Delta\Delta H_f^\circ$) of 6.31 kcal/mol for a 7.5° change in θ .

The MO energies for gauche 1,2-Ph-Ph interactions are shown in Figure 7, together with their corresponding wave functions. The orientation of the wave functions is changed with respect to that of the eclipsed conformation. The axis of the nodes separating the a_2 and b_1 orbitals is rotated to allow for maximal interaction of the b_1 orbitals at the C_2 - C_2 positions of the phenyl groups, not at the C_1 - C_1 positions as in the eclipsed conformation. The HOMO of the gauche conformation is analogous to that of the eclipsed conformation, with a large amount of hyperconjugation through the benzylic C-C σ bond. Again, due to symmetry considerations, the orbital energy is relatively unaffected by

changes in θ . The second highest HOMO of the gauche conformation is the b_1 - b_1 antisymmetric combination orbital. The energy of this orbital is decreased relative to the eclipsed conformation, signifying a slight decrease in the amount of through-space interaction observed. Because of the initial decrease in the through-space interactions, a greater change in θ is required before this orbital becomes the HOMO for $\theta < 107^\circ$.

Discussion

Assignment of the Observed Rates to Electron-Transfer Processes. The assignment of these rate constants to originate from et processes is supported by several considerations. The reaction is kinetic first-order in both **1** and $\text{Fe}^{\text{III}}\text{L}_3$. Product studies show that the reaction has the proper stoichiometry for an initial single electron-transfer reaction.²⁰ The constancy of the observed rates as a function of both the concentration of added base and the structure of the added base indicates that the reaction is not base-catalyzed. The fact that only ketone products are formed in the reaction, coupled with the independence of the rate from structural features of the added base, does not allow an acid-catalyzed reaction pathway. An alternative mechanism involving a rate-determining homolysis of **1** followed by fast oxidation of the corresponding radicals is ruled out by an experimentally determined ΔG_{30}^\ddagger of 32.3 kcal/mol for homolytic cleavage,²⁴ compared to the observed ΔG_{30}^\ddagger of 22.1 kcal/mol for the present reaction.

Further support for the et nature of the reaction comes from comparison of the ΔG_{30}^\ddagger data shown in Table II with the calculated ΔG_{30}° values shown in Table III. The reaction of **1a** with $\text{Fe}^{\text{III}}\text{L}_3$ has a calculated ΔG_{30}° and an experimentally determined ΔG_{30}^\ddagger of 18.2 and 22.1 kcal/mol, respectively. The agreement of these values is surprisingly good, given that the calculation of ΔG_{30}° requires the assumption that the solvation energetics of **1** are similar in magnitude to those of the monoaryl systems where the correlation of IP and E_{ox}° data was developed. The fact that $\Delta G^\ddagger > \Delta G^\circ$ for this reaction is consistent with the expectation that ΔG^\ddagger should be $\geq \Delta G^\circ$ for any endergonic reaction. A similar comparison of the calculated ΔG_{30}° and the experimentally determined ΔG_{30}^\ddagger for **1e** yields 17.0 and 20.2 kcal/mol, respectively, in complete agreement with our arguments concerning **1a**.

The interpretation of the results being due solely to et processes hinges upon the assumption that the rate of back electron transfer (k_{bet}) does not compete with the rate of bond cleavage (k_c). An approximate limit to the height of the barrier separating the radical cation from cleavage products may be obtained from the lifetime of 1,1,2,2-tetra-*p*-anisyl-1,2-ethanediol radical cation (**1f⁺**) of 66 ps,¹⁷ corresponding to a ΔG^\ddagger of 3.6 kcal/mol at room temperature.²⁵ Since **1f⁺** may be expected to be the most stabilized **1⁺** and would result in the most stabilized intermediates, the ΔG^\ddagger (**1f⁺**) of 3.6 kcal/mol must be considered to be an upper limit to the cleavage barrier of **1⁺**. The isomers of **1** included in this study must have somewhat lower barriers. The measured ΔG^\ddagger for **1a** is more than 3.6 kcal/mol greater than the predicted $\Delta G_{\text{et}}^\circ$ for the same reaction, signifying an energy preference for the cleavage reaction relative to back electron transfer. The reaction preference for **1e⁺** is not quite so clear, since the difference between the measured ΔG^\ddagger and the predicted $\Delta G_{\text{et}}^\circ$ is somewhat less than the 3.6 kcal/mol estimate of the **1e⁺** bond-cleavage energy. In this case, k_{bet} may be comparable to k_c . Although the exact value of the k_{et} is less certain for **1e**, our overall assertion that the oxidation potential of **1** is less than predicted is unaffected. If the bond-cleavage energy is greater than the energy required for back et, the $\Delta G_{\text{et}}^\ddagger$ must be less than the observed ΔG^\ddagger . We conclude that the k_{et} presented here are minimum values and that the $\Delta G_{\text{et}}^\ddagger$ presented here represent maximum values.

Comparison of 1 Electron-Transfer Energetics to Model Systems. The results obtained here indicate that the isomers of **1**

(24) Weiner, S. A. *J. Am. Chem. Soc.* **1971**, *93*, 6978.

(25) These data are subject to the limitations discussed below. A stabilized **1f⁺** would be expected to undergo slower back electron transfer. Therefore, the estimated ΔG_c^\ddagger (**1f⁺**) is a lower limit, further increasing our confidence that the observed rates correspond to et processes.

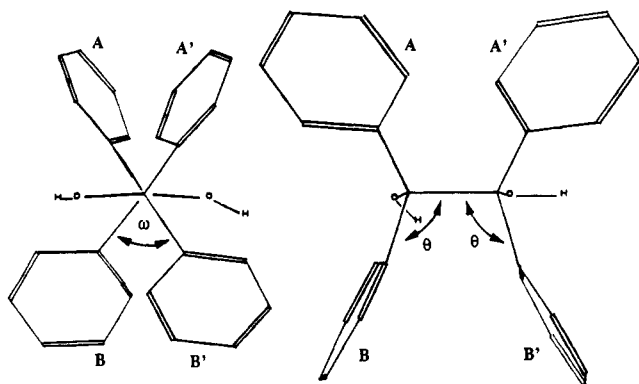


Figure 8. X-ray crystal structure of **1a** shown in perpendicular views.

included in this study undergo et more easily than expected in both the gas phase and solution. In order to simplify the discussion, we will focus on the gas-phase IP data. The IP(**1a**) = 8.42 eV that **1a** is oxidized more easily than toluene or *tert*-butylbenzene (IP = 8.65 eV).^{22,26} Additional alkyl substitution on arenes is well-known to lower the IP.²⁶ Therefore, the reduced IP(**1a**) indicates that **1a** is oxidized as easily as 1,3,5-trimethylbenzene (IP = 8.42 eV),²² even though only a single alkyl group is attached to each phenyl group of **1a**.

The good agreement of the IP and ΔG_{et}^{\ddagger} data for **1a,e** argues that there is a unique molecular property of these compounds that leads to easy oxidation. One potential rationale for the reduced IP is the interaction of the oxygen lone-pair electrons with the phenyl π orbitals. Such interactions have been invoked to rationalize the enhanced acidity of pentaphenylhydroxyethanes relative to triphenylhydroxymethanes.²⁷ However, this type of interaction appears to be unimportant in reducing the IP of **1**. Since **3** should have similar steric interactions as may be found in **1**, the enforced oxygen lone-pair interactions with the phenyl π systems should be similar in **1** and **3**. However, the large difference in the IP between **1a** and **3** (0.59 eV) makes it impossible to believe that this effect is responsible for the easy oxidation of **1**. Therefore, Ph-Ph interactions are responsible for the decreased IP of **1**.

Origin of Ph-Ph Interactions. While there is no doubt that enforced Ph-Ph interactions in rigid cyclic systems (e.g., cyclophanes)^{28,29} can lead to IP and E_{ox}° decreases similar to those observed in this study, the evidence concerning the existence of Ph-Ph interactions in acyclic systems is much less certain. Several groups have observed that the UPS spectra of diphenylmethane³⁰⁻³² or 1,2-diphenylethane³² are identical with that of toluene, indicating no significant interaction of the phenyl groups in these molecules. However, ESR observations of methylarene³³ or anthryl³⁴ radical cations indicate that complexation of the radical cation with a neutral molecule gives stabilization of the odd electronic charge. These conflicting data indicate that any postulate of Ph-Ph interactions in acyclic systems must be supported by experimental data. Since the theoretical calculations reported here (vide supra) indicate that both 1,1-Ph-Ph interactions and 1,2-Ph-Ph interactions may cause a decrease in the IP, we have

attempted to evaluate the origin of the decreased IP in **1** by two different methods. The first method was to examine the X-ray crystal structure for possible interaction modes. The second method was to experimentally evaluate k_{et} for specifically substituted isomers of **1**.

The X-ray crystal structure of **1a** has been recently determined and is shown in Figure 8.³⁵ Two alternative views of the molecule are presented for the sake of clarity. The view on the left is essentially a Newman projection of the structure, by viewing down the axis of the benzylic C-C σ bond. The view on the right has been rotated by 90° to view the interactions of the A, A'- and B, B'-phenyl groups. Although the X-ray crystal structure suffers from some disorder in the positions of the benzylic carbons and the OH bonds in **1a**, the relative relationship of the phenyl groups to each other should not be affected by this disordering and will serve to show the relative geometries of the aryl groups to each other. Supporting evidence that the X-ray crystal structure is similar to the gas-phase and to the solution-phase structures comes from the similarity of the AM-1 minimum-energy structure of **1a** to the X-ray crystal structure.

The four phenyl groups of **1a** can be divided into two sets of equivalent groups, labeled A and B in Figure 8. The A, A'-phenyl groups can be seen to be nearly at right angles to the B, B'-phenyl groups. In this geometry, there can be NO 1,1-Ph-Ph interactions, because the A- and B-phenyl groups and the A'- and B'-phenyl groups are oriented at right angles to each other. This geometry forces the hydrogens of the A-phenyl group into the π face of phenyl group B, causing θ to be decreased to 103.5°. A similar interaction occurs between the A'- and the B'-phenyl groups. These steric interactions force a face-to-face interaction of the two B-phenyl groups. We note that significant IP decreases were observed in the model calculations for both the eclipsed and the gauche conformations using this value for θ . A further point about the crystal structure geometry is that the interactions appear to be from a gauche geometry, since $\omega = 65^\circ$ in this structure. Therefore, if the et event occurs adiabatically from the lowest energy geometry, the X-ray crystal structure indicates that 1,2-Ph-Ph interactions through a gauche conformation are responsible for the observed IP decrease.

Supporting evidence for the importance of gauche 1,2-Ph-Ph interactions comes from the magnitude of the reduced IP for each additional methyl group of **1**. The ca. 0.4-eV decrease in the IP of toluene relative to benzene has been attributed to splitting of the $1e_{1g}$ orbitals of benzene into a b_1 orbital and an a_2 orbital.²⁶ In contrast, the four methyl groups of **1e** result in $\Delta IP = 0.07$ eV relative to **1a**. Each methyl substituent has only a minimal effect on ΔIP . Although a trivial explanation of this phenomenon is that only two aryl groups are responsible for the observed decreases, the steady decrease in ΔG_{et}^{\ddagger} for the series **1a-e** suggests that all aryl groups of **1** have similar importance. An empirical correlation has been developed²⁶ to estimate the IP decrease for the methyl substitution to aromatic compounds and is shown in eq 5. In this equation, $\Delta IP_{\nu,j}$ is the change in the IP for each

$$-\Delta IP_{\nu,j} = 0.0528 + 1.0110 \left(\sum_{\xi} \frac{3C_{J\xi}^2 + C_{J\tau}^2 + C_{J\tau'}^2}{3} \right) \quad (5)$$

molecular orbital energy due to the substituent, ξ is the position of methyl substitution, τ and τ' are the nearest-neighbor carbons, and C_{Jk} is the coefficient of the k th AO of the J th MO. With this equation and the AO coefficients derived from the bibenzyl calculations for $\theta = 100^\circ$, $\Delta IP = 0.19$ and 0.15 eV for the eclipsed and gauche conformations, respectively. Two points concerning these calculated data are important. First, the extended π system (originating from the through-space interactions) effectively decreases the coefficient of each AO in the MO wave function. The extended π system serves the function of decreasing the individual effect of each substituent. Second, the gauche conformation, with the HOMO rotated to give the maximal overlap at the C_2-C_2

(26) (a) Heilbronner, E.; Hornung, V.; Pinkerton, F. H.; Thames, S. F. *Helv. Chim. Acta* **1972**, *55*, 289. (b) Kobayashi, T.; Nagakura, S. *Bull. Chem. Soc. Jpn.* **1974**, *47*, 2563.

(27) Steward, W.; Fussaro, D. R. *J. Organomet. Chem.* **1977**, *120*, C28.

(28) Kovac, B.; Mohraz, M.; Heilbronner, E.; Boekelheide, V.; Hopf, H. *J. Am. Chem. Soc.* **1980**, *102*, 4314.

(29) Haenel, M. W.; Schweitzer, D. *Polynuclear Aromatic Compounds. Adv. Chem. Ser.* **1988**, *217*, 333.

(30) Klasinc, L.; Ruscic, B.; Sabljic, A.; Trinajstic, N. *J. Am. Chem. Soc.* **1979**, *101*, 7477.

(31) Eaton, D. F.; Traylor, T. G. *J. Am. Chem. Soc.* **1974**, *96*, 7109.

(32) Pignataro, S.; Mancini, V.; Ridyard, J. N. A.; Lempka, H. J. *J. Chem. Soc., Chem. Commun.* **1971**, 142.

(33) El-Shall, M. S.; Meot-Ner (Mautner), M. *J. Phys. Chem.* **1987**, *91*, 1088.

(34) Terahara, A.; Ohya-Nishiguchi, H.; Hirota, N.; Higuchi, H.; Misumi, S. *J. Phys. Chem.* **1986**, *90*, 4958.

(35) Bond, D. R.; Bourne, S. A.; Nassimbeni, L. R.; Toda, F. *J. Crystallogr. Spectrosc. Res.* **1989**, *19*, 809.

Table IV. Calculated Rate Contributions for 1,1- and 1,2-Phenyl-Phenyl Interactions^a

compound	k_{et}^b	k_{et}^c
1a	$2k_{pp}$	$2k_{pp}$
1b	$k_{PT} + k_{PP}$	$k_{PT} + k_{PP}$
1c	$2k_{PT}$	$2k_{PT}$
1d^d	$1/2(2k_{PT} + 2k_{PT})$	$1/2(2k_{PT} + k_{PP} + k_{TT})$
1e	$2k_{TT}$	$2k_{TT}$

^a Key: k_{pp} , rate for a single phenyl-phenyl interaction; k_{PT} , rate for a single phenyl-tolyl interaction; k_{TT} , rate for a single tolyl-tolyl interaction. ^b Assuming that only 1,1-phenyl-phenyl interactions are important. ^c Assuming that only 1,2-phenyl-phenyl interactions are important. ^d Calculated for the 50:50 diastereomeric mixture.

positions, gives a smaller ΔIP for each methyl substituent than the eclipsed conformation. Therefore, the diminished ΔIP for methyl substitution is consistent with 1,2-Ph-Ph interactions, preferably through the gauche conformation.

Although the X-ray crystal structure of the molecule argues strongly that 1,2-Ph-Ph interactions are responsible for the decrease in the IP, conformational changes prior to the et (i.e., nonadiabatic et) may still result in 1,1-Ph-Ph interactions being more important than 1,2-interactions. For this purpose, we have attempted to obtain experimental evidence relating to the relative importance of the 1,1- or 1,2-Ph-Ph interactions. Since the experimental uncertainties of the IP as derived from UPS are quite large, we have measured k_{et} for **1b-d**, which have only 5% error limits. **1c** was synthesized in order to examine the effect of 1,1-Ph-Ph interactions, while **1d** was synthesized to examine the effect of 1,2-Ph-Ph interactions. **1b** was added to evaluate the effects of a single tolyl group on k_{et} .

A detailed analysis of the effective reaction rates is given below. The symmetry of the molecule dictates that two possible interactions must be considered in each molecule to determine the overall rate of reaction. For 1,2-Ph-Ph interactions, the X-ray crystal structure of Figure 8 shows that two possible interactions occur in each molecule. The same situation would occur for 1,1-Ph-Ph interactions, since both ends of the molecule would be expected to contribute to the overall rate. We have given the overall rate anticipated from each substituted isomer of **1** in Table IV. Therefore, $k_{et}(\mathbf{1a})$ will be the sum of two Ph-Ph interactions ($2k_{pp}$), regardless of whether 1,1- or 1,2-interactions are the important Ph-Ph interaction mode. Similarly, $k_{et}(\mathbf{1e})$ must be made up of two tolyl-tolyl interactions ($2k_{TT}$), while **1b** must originate from a Ph-Ph interaction and a phenyl-tolyl interaction ($k_{pp} + k_{PT}$). The differentiation between 1,1- and 1,2-interactions must come from a comparison of $k_{et}(\mathbf{1c})$ and $k_{et}(\mathbf{1d})$. $k_{et}(\mathbf{1c})$ either will be controlled by a tolyl-tolyl and a Ph-Ph interaction if 1,1-interactions are important or will be due to two phenyl-tolyl interactions if 1,2-interactions are important. For **1d**, the situation is more complicated because of the use of the diastereomeric mixture.³⁶ For *meso*-**1d**, two phenyl-tolyl interactions are observed, regardless of whether 1,1- or 1,2-Ph-Ph interactions are important. In contrast, the *d,l*-**1d** pair will have different rates, dependent on whether 1,1-interactions ($2k_{PT}$) or 1,2-interactions ($k_{pp} + k_{PT}$) are important.

In the present study, k_{et} at 30 °C are listed in Table II. From these relative rates and the rate contributions anticipated for **1a,b,e** (Table IV), relative values of k_{pp} , k_{PT} , and k_{TT} are easily evaluated to be 0.55, 2.55, and 13.4, respectively. As seen in Table IV, the calculated rate for **1c** would be 5.1, regardless of whether 1,1- or 1,2-Ph-Ph interactions are responsible for the observed reaction dynamics, in reasonable agreement with our observed rate of 6.0. For a 50:50 mixture of **1d**, calculated rates of 5.1 or 9.5 are obtained for 1,1- or 1,2-Ph-Ph interactions, respectively. Although the similarity of $k_{et}(\mathbf{1d})$ to $k_{et}(\mathbf{1c})$ and to the predicted reaction rate for 1,1-Ph-Ph interactions would seem to argue that 1,1-

Ph-Ph interactions were more important than 1,2-Ph-Ph interactions, we hesitate to make a definitive assignment because of our inability to verify that **1d** is a 50:50 mixture of diastereomers and because of the weak relative effect of each substituent on the IP or the E_{ox}° .

In summary, we favor the rationale that 1,2-Ph-Ph interactions are responsible for the decrease in IP for **1** because of the excellent agreement of the gas-phase IP and the solution-phase E_{ox}° indicating a similar structure for the electron-transfer event in both phases. Since our theoretical calculations predict that the orientation of the phenyl groups in the crystal structure should have significant through-space interactions leading to an IP decrease similar to that observed experimentally, we prefer the assignment that the 1,2-Ph-Ph interactions are responsible for the observed ease of the electron transfer. However, the similarity in rates between **1c,d** makes it impossible to rule out 1,1-Ph-Ph interactions being more important for rationalizing the observed behavior.

Implications of the Reduced IP Data. A large number of studies have been concerned with understanding of the factors involved in bond cleavage via photoinitiated charge transfer.¹⁻⁴ A common assumption in the quantitative data analysis of reaction mechanisms is that the rate of back electron transfer is similar for structurally similar compounds. The results obtained in this study suggest that diaryl interactions may significantly affect the energetics of the radical cations formed by the et event. Since k_{bet} is expected to be strongly influenced by the ΔG_{bet}° , changes in the radical-cation energies will change the ΔG_{bet}° , which may significantly alter k_{bet} .

For example, in addition to a number of other compounds, Kochi¹⁷ has recently advocated the use of tetra-*p*-anisylethanediod (**1f**) as a "radical cation clock". The time constant of this "clock" was evaluated by measuring the quantum yield of photoinitiated et from **1f** to chloranil (CA) and by assuming that k_{bet} from the chloranil radical anion (CA⁻) to **1f**⁺ was identical with the k_{bet} for CA⁻ to the *p*-methoxytoluene radical cation (MT⁺). If **1f** has aryl-aryl interactions similar to those of the other isomers of **1** studied here, then ΔG_{bet}° for CA⁻ to **1a**⁺ will be quite different from the ΔG_{bet}° for CA⁻ to MT⁺.

In order to verify this change in radical-ion energetics, we have attempted to evaluate k_{et} for **1f** to Fe^{III}L₃ under conditions analogous to those reported here. This rate would allow a determination of ΔG_{et}° for the reaction of **1f** and Fe^{III}L₃ and would therefore provide an estimate of the ΔG_{et}° for the same reaction. These data could then be compared to the known data for the reaction of MT to Fe^{III}L₃, which have been reported to have $k_{et} = 6 \text{ M}^{-1} \text{ s}^{-1}$ ($\Delta G^{\circ} = 13.9 \text{ kcal/mol}$).^{13b} However, under all conditions employed by us, including initial concentrations of both Fe^{III}L₃ and **1f** of 10⁻⁴ M, the oxidation reaction proceeded in less than 1 min. If we assume that complete reaction occurred in 1 min at these concentrations, an extremely conservative lower limit for k_{et} is $\geq 166 \text{ M}^{-1} \text{ s}^{-1}$ ($\Delta G^{\circ} \leq 9 \text{ kcal/mol}$). Although all the control experiments have not been performed to definitely prove that the reaction of **1f** and Fe^{III}L₃ proceeds by an outer-sphere et mechanism analogous to the reactions observed in this study, these results strongly suggest that **1f**⁺ is significantly more stable than MT⁺. The enhanced stability of **1f**⁺ is likely to affect the overall dynamics of any subsequent reactions, making strictly quantitative estimates of reaction rates difficult.

These results also have significance in the analysis of the temperature dependence of the photoinitiated bond-cleavage quantum yields from which radical-cation cleavage activation energies are derived.^{1a,2c} While the uncertainties associated with the temperature dependence of k_{bet} are severe enough, the current study makes questionable the assumption that the ΔG_{bet} between seemingly similar molecules are equivalent. For example, ΔG_{bet} for erythro isomers may be markedly different from ΔG_{bet} for threo isomers, depending on the conformation at the time of electron transfer^{2c} and whether significant Ph-Ph interactions occur after the et event. Alternatively, a change from monophenyl substitution to diphenyl substitution may be sufficient to alter the energetics significantly by opening new pathways for Ph-Ph interactions. Further studies into the alteration of the radical-cation energetics

(36) In our hands, the diastereomeric mixture was completely inseparable. Identical HPLC and GC retention times on a variety of columns were obtained. In addition, identical NMR signals ruled out attempted partial-reaction experiments to determine whether one isomer reacted faster than the other. Therefore, we can only present an overall observed rate for **1d**.

are currently in progress in our laboratories to evaluate potential aryl-aryl interactions and their effects on the ease of radical cation formation.

Experimental Section

Melting points were determined on a Laboratory Devices Mel-Temp apparatus and are uncorrected. Gas-liquid chromatographic analyses were conducted on a Hewlett-Packard Model 5890A GLC equipped with a 10-m 5% phenylmethylsilicone or a Carbowax 20M Megabore column. HPLC was performed on a Waters Associates Protein Peptides I system capable of gradient elution and with UV detection at 254 nm. Integration of the signals was performed by a Hewlett-Packard Model 3390A digital integrator. GCMS were measured with a Finnigan Model 4021 quadrupole mass spectrometer equipped with a Model 9610 data reduction system for comparison of mass spectra to those of authentic samples. IR spectra were recorded on a Perkin-Elmer Model 1310 IR spectrophotometer. ^1H NMR spectra (δ (ppm) and J (Hz)) were measured in the indicated solvent with TMS as an internal standard on a Varian Instruments EM-360 or a JEOL-GX-270 NMR spectrometer. UV-vis spectra were measured with a DMS-100 spectrophotometer.

Acetonitrile was predried over CaH_2 and then distilled from P_2O_5 shortly before use. Benzophenone was purchased from Aldrich. 4-Methylbenzophenone and 4,4'-dimethylbenzophenone were prepared by the method of Yamataka et al.³⁷

1,1,2,2-Tetraphenylethanedione (1a). A saturated solution of benzophenone in isopropyl alcohol was prepared by allowing excess benzophenone to dissolve over several days in isopropyl alcohol. The excess benzophenone was removed by vacuum filtration. The solution was placed in a quartz tube and irradiated for 48 h with 300-nm light from a Rayonet reactor. Following solvent removal in vacuo, the crude product was crystallized 3 \times from hexane/ethyl acetate to give colorless crystals, mp 185–188 $^\circ\text{C}$ (lit.³⁸ mp 188–190 $^\circ\text{C}$).

Tetratolyethanedione (1e). A procedure similar to that for **1a** was used to produce colorless crystals of **1e**, mp 174–175 $^\circ\text{C}$ (lit.³⁹ mp 175–177 $^\circ\text{C}$).

1,2,2-Triphenyl-1-tolyethanedione (1b). To a 50-mL solution of anhydrous diethyl ether and 1.05 g of benzil (5.0 mmol) at 0 $^\circ\text{C}$ was added dropwise 1.7 mL of 3 M phenylmagnesium bromide (Aldrich). The solution was allowed to warm to room temperature and stirred for 2 h. The reaction mixture was poured into an aqueous ammonium chloride solution. The organic layer was separated, and the aqueous layer was extracted 2 \times with ether. After the ether portions were combined, the solution was dried (Na_2SO_4) and the solvent removed in vacuo. The crude product was isolated from silica gel chromatography (hexane/ethyl acetate) to yield 1-hydroxy-1,1,2-triphenyl-2-ethanone, mp 81–83 $^\circ\text{C}$ (lit.⁴⁰ mp 84–85 $^\circ\text{C}$). This product was reacted in a similar fashion with *p*-tolylmagnesium bromide to yield crude **1b**, which was recrystallized 3 \times from hexane/ethyl acetate to yield colorless crystals: mp 172–174 $^\circ\text{C}$; ^1H NMR (CDCl_3) δ 2.31 (s, 3 H), 3.06 (s, 2 H), 7.2 (m, 19 H). Anal. Calcd for $\text{C}_{27}\text{H}_{24}\text{O}_2$: C, 85.23; H, 6.36. Found: C, 85.01; H, 6.36.

(37) Yamataka, H.; Fujimura, N.; Kawafuji, Y.; Hanafusa, T. *J. Am. Chem. Soc.* **1987**, *109*, 4305.

(38) Blatt, A. H. *Organic Synthesis*; Wiley: New York, **1943**; Collect. Vol. II, 71.

(39) Gomberg, M.; Bachmann, W. E. *J. Am. Chem. Soc.* **1927**, *49*, 236.

(40) Trzuppek, L. S.; Newirth, T. L.; Kelly, E. G.; Sbarbati, N. E.; Whitesides, G. M. *J. Am. Chem. Soc.* **1973**, *95*, 8118.

1,2-Diphenyl-1,2-ditolyethanedione (1d). To a 50-mL solution of anhydrous diethyl ether and 1.05 g of benzil (5.0 mmol) at 0 $^\circ\text{C}$ was added dropwise 1.0 mL of 1.0 M *p*-tolylmagnesium bromide. The solution was allowed to warm to room temperature with stirring for 2 h and poured into aqueous ammonium chloride. After extraction 3 \times with ether, the ether extracts were combined and dried (Na_2SO_4). Solvent removal in vacuo followed by recrystallization 3 \times from hexane/ethyl acetate yielded colorless crystals, mp 173–175 $^\circ\text{C}$ (lit.³⁹ mp 173–175 $^\circ\text{C}$).

1,1-Diphenyl-2,2-ditolyethanedione (1c). To 15 mL of isopropyl alcohol were added 0.5 g of benzophenone (1.4 mmol) and 0.54 g of 4,4'-dimethylbenzophenone (1.4 mmol). This solution was placed in a quartz tube and irradiated with the 300-nm light of a Rayonet reactor for 48 h. Solvent removal in vacuo gave crude product, which showed **1a,c,e** to be present in a 1:1:1 ratio by HPLC. The crude products were partially separated by silica-gel column chromatography (hexane/ethyl acetate). The fractions containing **1c** as the major product were fractionally crystallized from acetonitrile to give pure **1c** as determined by HPLC analysis: mp 174–176 $^\circ\text{C}$; ^1H NMR (CDCl_3) δ 2.29 (s, 6 H), 3.00 (s, 2 H), 7.2 (m, 18 H).

Product Determinations. A solution of **1d** or **e** (0.01 M), DBP (2.5 mM), and $\text{Fe}^{\text{III}}(1,10\text{-phen})_3(\text{ClO}_4)_3$ (0.5 mM) in CH_3CN was prepared. After three freeze-pump-thaw degassing cycles, the reaction mixture was stirred at the indicated temperature for the indicated time. The products were identified by their identical HPLC retention times. Quantitative analysis of the reaction mixture was accomplished with phenyl benzoate as an internal standard. The results are gathered in Table I.

Electron-Transfer Rate Determinations. In a typical kinetic experiment, separate solutions of $\text{Fe}^{\text{III}}\text{L}_3$, a mixture of the added base (i.e., DBP or 4CP), and **1** were dissolved in freshly distilled CH_3CN (from P_2O_5) and degassed by three freeze-pump-thaw cycles. After sealing under vacuum, the solutions were brought to the temperature of the experiment and mixed immediately prior to the beginning of observation to give final concentrations of $[\text{Fe}^{\text{III}}\text{L}_3] = 5 \times 10^{-4}$ M, $[\text{base}] = 2.5 \times 10^{-3}$ M, and $[\mathbf{1}] = 0.01$ M. The concentrations of $\text{Fe}^{\text{II}}\text{L}_3$ and $\text{Fe}^{\text{III}}\text{L}_3$ were monitored at 506 and 630 nm, respectively. All kinetic experiments were followed for a minimum of 3 half-lives and had a correlation coefficient of 0.998 to be included in the data set.

UPS Spectral Determinations. Photoelectron spectra were measured at the University of Cologne with a Leybold-Heraeus UP spectrometer (Model UPG200). The energy scale was calibrated with Ar (Ar $2p_{3/2} = 15.76$ eV) and Xe (Xe $4p_{3/2} = 12.13$ eV). Small amounts of Ar were added to each sample to monitor instrumental drift. All spectra were obtained with He I excitation ($h\nu = 21.2$ eV).

Theoretical Calculations. The AMPAC 1.00 package⁴¹ was used for calculation of the IPs. Initial geometries were generated with the programs CHEMCAD or PCMODEL and transferred to a VAX-8650 for energy minimization.

Acknowledgment. We gratefully acknowledge the financial support of the Gas Research Institute (Contract No. 5085-260-1177) in order to complete this work. We also gratefully acknowledge Professor Georg Hohlneicher and his group at the Universität zu Köln for measurements of the gas-phase UPS spectra and Professor Vernon Parker and his group at Utah State University for $E_{\text{ox(p)}}$ data for **1a** and **3**.

(41) QCPE No. 506. *QCPE Bull.* **1986**, *6*, 24a.